JCI The Journal of Clinical Investigation

# Band 3 and glycophorin are progressively aggregated in density-fractionated sickle and normal red blood cells. Evidence from rotational and lateral mobility studies.

J D Corbett, D E Golan

*J Clin Invest.* 1993;91(1):208-217. https://doi.org/10.1172/JCI116172.

**Research Article**

Band 3 aggregation in the plane of the red blood cell (RBC) membrane is postulated to be important in the pathophysiology of hemolysis of dense sickle and normal RBCs. We used the fluorescence photobleaching recovery and polarized fluorescence depletion techniques to measure the lateral and rotational mobility of band 3, glycophorins, and phospholipid analogues in membranes of density-separated intact RBCs from seven patients with sickle cell disease and eight normal controls. The fractions of laterally mobile band 3 and glycophorin decreased progressively as sickle RBC density increased. Normal RBCs also showed a progressive decrease in band 3 fractional mobility with increasing buoyant density. Rapidly rotating, slowly rotating, and rotationally immobile forms of band 3 were observed in both sickle and normal RBC membranes. The fraction of rapidly rotating band 3 progressively decreased and the fraction of rotationally immobile band 3 progressively increased with increasing sickle RBC density. Changes in the fraction of rotationally immobile band 3 were not reversible upon hypotonic swelling of dense sickle RBCs, and normal RBCs osmotically shrunken in sucrose buffers failed to manifest band 3 immobilization at median cell hemoglobin concentration values characteristic of dense sickle RBCs. We conclude that dense sickle and normal RBCs acquire irreversible membrane abnormalities that cause transmembrane protein immobilization and band 3 aggregation. Band 3 aggregates could serve as cell surface […]



# Band 3 and Glycophorin Are Progressively Aggregated in Density-fractionated Sickle and Normal Red Blood Cells

## Evidence from Rotational and Lateral Mobility Studies

**James D. Corbett and David E. Golan**
*Departments of Biological Chemistry and Molecular Pharmacology, and Medicine, Harvard Medical School, Hematology-Oncology Division, Brigham and Women's Hospital, Boston, Massachusetts 02115*

## Abstract

**Band 3 aggregation in the plane of the red blood cell (RBC) membrane is postulated to be important in the pathophysiology of hemolysis of dense sickle and normal RBCs. We used the fluorescence photobleaching recovery and polarized fluorescence depletion techniques to measure the lateral and rotational mobility of band 3, glycophorins, and phospholipid analogues in membranes of density-separated intact RBCs from seven patients with sickle cell disease and eight normal controls. The fractions of laterally mobile band 3 and glycophorin decreased progressively as sickle RBC density increased. Normal RBCs also showed a progressive decrease in band 3 fractional mobility with increasing buoyant density. Rapidly rotating, slowly rotating, and rotationally immobile forms of band 3 were observed in both sickle and normal RBC membranes. The fraction of rapidly rotating band 3 progressively decreased and the fraction of rotationally immobile band 3 progressively increased with increasing sickle RBC density. Changes in the fraction of rotationally immobile band 3 were not reversible upon hypotonic swelling of dense sickle RBCs, and normal RBCs osmotically shrunken in sucrose buffers failed to manifest band 3 immobilization at median cell hemoglobin concentration values characteristic of dense sickle RBCs. We conclude that dense sickle and normal RBCs acquire irreversible membrane abnormalities that cause transmembrane protein immobilization and band 3 aggregation. Band 3 aggregates could serve as cell surface sites of autologous antibody binding and thereby lead to removal of dense sickle and normal (senescent) RBCs from the circulation. (*J. Clin. Invest.* 1993. 91:208–217.) Key words: fluorescence photobleaching recovery • fluorescence recovery after photobleaching • hemolysis • polarized fluorescence depletion • Stractan gradient**

## Introduction

Cell membranes are transducers by which intracellular events affect interactions of the cell with its extracellular environment. The primary pathophysiological event in sickle cell disease, polymerization of hemoglobin S within sickle red blood cells (RBCs),[1] leads to alterations in sickle RBC membranes that enhance interactions between sickle RBCs and bone marrow–derived mononuclear phagocytes (1). These interactions are likely to lead to premature removal of sickle RBCs from the circulation, a major clinical problem in sickle cell disease.

The normal RBC membrane is composed of a lipid bilayer, in which integral membrane proteins are embedded, and a multicomponent protein skeleton, which laminates the inner bilayer surface (2). Two major integral membrane glycoproteins, band 3 and glycophorin A, span the bilayer. Band 3, present in $\sim 10^6$ copies per cell (3), mediates anion exchange across the membrane (4). Glycophorin A, present in $\sim 5 \times 10^5$ copies per cell (5), is the major sialoglycoprotein. The membrane skeleton determines RBC stability, deformability, and shape (6–9) and appears to regulate lateral and rotational mobility of band 3 and glycophorin A in the plane of the membrane (10–18). The major skeletal protein, spectrin, is attached to the overlying bilayer through interactions involving: ankyrin, which links spectrin to a portion (10–15%) of band 3; protein 4.1, which links spectrin to glycophorin C and possibly to glycophorin A and band 3; and, possibly, inner leaflet aminophospholipids, including phosphatidylserine and phosphatidylethanolamine (2).

Sickle RBC membranes exhibit multiple structural and functional abnormalities (for review see reference 19). Irreversibly sickled cells (ISCs) are abnormally rigid (20) and manifest increased exposure of aminophospholipids in the outer leaflet of the RBC membrane (21–25). Membrane skeletons from ISCs retain the deformed sickle shape in the absence of hemoglobin and membrane lipid (26). Negative charges at the surface of sickle RBCs, presumably carried by glycophorins, may be abnormally clustered (27, 28), although this finding is controversial (29). Elevated levels of hemoglobin are found at the inner surface of sickle RBC membranes, presumably bound to band 3 (30). Sickle RBC membranes have increased lipid peroxidation (31) and intraprotein disulfide bonds (1) as manifestations of oxidant damage induced by increased levels of activated oxygen products (32; for review see reference 33). Finally, sickle RBCs exhibit net potassium and water loss (34, 35) and net calcium accumulation (36). These changes are progressive over the life span of the cell.

Address correspondence to David E. Golan, M.D., Ph.D., Department of Biological Chemistry and Molecular Pharmacology, Harvard Medical School, 250 Longwood Avenue, Boston, MA 02115.

*Received for publication 8 June 1992 and in revised form 20 August 1992.*

J. Clin. Invest.

0021-9738/93/01/0208/10 $2.00
Volume 91, January 1993, 208–217

1. *Abbreviations used in this paper:* EMA, eosin maleimide; Fl-PE, fluorescein phosphatidylethanolamine; FPR, fluorescence photobleaching recovery; FTSC, fluorescein thiosemicarbazide; ISC, irreversibly sickled cell; KPBS, high potassium phosphate-buffered saline; MCHC, median cell hemoglobin concentration; PFD, polarized fluorescence depletion; PMT, photomultiplier tube; RBC, red blood cell; RSC, reversibly sickled cell.

Many RBC membrane defects are also found in normal cells of increased density. Membrane surface area is decreased (37), with nonselective loss of phospholipid, cholesterol (38), and sialic acid bearing glycoproteins (39, 40) (but not band 3). Cell deformability is impaired. Activities of many cellular enzymes are decreased, including glycolytic enzymes, superoxide dismutase (41), glutathione peroxidase (42), and glutathione reductase; ATP levels are normal, however. Increased oxidized glutathione (42) and membrane-associated hemoglobin (43) and hemichrome (44) may indicate that progressive oxidative membrane damage occurs with increasing cell age (33). Increased clustering of cell surface negative charges (45) and increased cell surface binding of autologous IgG (46–51) are also found in dense normal cells.

Changes at the RBC surface are likely to be responsible for the observed increase in hemolysis of dense sickle and normal cells. Cell surface changes could induce increased binding of autologous IgG to dense sickle and normal RBCs and thereby mediate the removal of such cells from the circulation (52–57). In this report we have used the techniques of fluorescence photobleaching recovery (FPR) and polarized fluorescence depletion (PFD) to measure the lateral and rotational mobility of band 3 and the lateral mobility of glycophorins and phospholipid analogues in membranes of density fractionated sickle and normal RBCs. Cell density correlates to some extent with cell age (58) and with sickle RBC morphology. By characterizing the physical state of band 3 and glycophorins in dense sickle and normal cells, we have elucidated molecular rearrangements that could directly mediate the removal of such cells from the circulation. Our data are consistent, on a molecular level, with the hypothesis that aggregates of band 3 serve as the primary binding site for autologous IgG and therefore as the likely cell surface signal for dense cell removal.

## Methods

Fluorescein phosphatidylethanolamine (Fl-PE) was obtained from Avanti Polar Lipids, Inc. (Alabaster, AL). Eosin maleimide (EMA) and fluorescein thiosemicarbazide (FTSC) were purchased from Molecular Probes, Inc. (Eugene, OR). Glucose oxidase, catalase, and Stractan were obtained from Sigma Chemical Co. (St. Louis, MO). After informed consent was obtained, fresh blood was collected by venipuncture into heparinized tubes. The buffy coat was immediately removed by aspiration and RBCs were washed three times and stored at 4°C in the following high potassium phosphate-buffered saline (KPBS) (mM): 140 KCl, 15 $NaPO_4$, 10 glucose, pH 7.4. High potassium buffers were used to prevent possible cellular dehydration associated with deoxygenation and fluorescent labeling.

*Labeling of RBC band 3.* 100 μl of freshly washed packed RBCs were incubated with 40 μl of EMA, 0.25 mg/ml in KPBS, at room temperature for 12 min. Cells were then washed three times in KPBS with 1% BSA. Under these labeling conditions > 80% of the membrane associated fluorescence was covalently bound to band 3.

*Labeling of RBC glycophorins.* 100 μl of freshly washed packed RBCs was incubated with 100 μl of $NaIO_4$, 2 mM in KPBS without glucose, at 4°C for 15 min. Cells were then washed twice in KPBS with 0.1 M glycerol and once with KPBS. 100 μl of oxidized RBCs was added to 100 μl of FTSC, 0.5 mg/ml in KPBS, at 4°C for 1 h. Labeled cells were washed three times in KPBS with 1% BSA. Under these conditions > 80% of the membrane-associated fluorescence was covalently bound to RBC sialoglycoproteins (glycophorins); of this amount 75% was bound to glycophorin A. FPR experiments on FTSC-labeled RBCs therefore measured the average lateral mobility of all RBC membrane glycophorins, although the major molecular species contributing to this measurement was glycophorin A.

*Labeling of RBCs with a fluorescent phospholipid analogue.* 20 μl of Fl-PE, 1 mg/ml in chloroform, was dried, resuspended in 0.5 ml of KPBS, and sonicated for 20 min in a low power bath sonicator. 100 μl of freshly washed packed RBCs was incubated with the Fl-PE solution at room temperature for 30 min. Cells were then washed three times in KPBS with 1% BSA.

*Separation of RBCs according to buoyant density.* Discontinuous Stractan density gradients (59) were used to separate sickle and normal RBCs into six different density fractions. Gradients were prepared as described by Galili et al. (52). Five 1.5-ml solutions of Stractan, with densities of 1.081, 1.085, 1.094, 1.107, and 1.111 g/ml, were layered on a cushion of 1.160 g/ml density in 15-ml ultracentrifuge tubes. Packed, washed RBCs were resuspended in 5 vol of KPBS containing 20 mM glucose, adjusted to pH 7.4 and 290 mosM as needed (KPBS/glucose), layered on the Stractan gradient, and centrifuged at 20,000 rpm in a rotor (SW40Ti; Beckman Instruments, Fullerton, CA) at 0°C for 30 min. RBC band 3 and glycophorins were fluorescently labeled before centrifugation on Stractan density gradients, whereas Fl-PE was incorporated into intact RBC membranes either before or after centrifugation. Successive RBC fractions were harvested from the gradient using a Pasteur pipette and washed five times in KPBS/glucose with 1% BSA. Unless otherwise indicated, RBCs from the 1.081–1.085 (band 2), 1.094–1.107 (band 4), and 1.111–1.160 (band 6) g/ml interfaces were used in FPR and PFD experiments. These fractions had median cell hemoglobin concentrations (MCHCs) of 30, 37, and 42 g/dl as measured by using the H1 system (Technicon Instruments Corp., Tarrytown, NY). Median rather than mean values were used, since the distributions of individual cell hemoglobin concentrations were non-Gaussian in each of the density fractions. In agreement with the results of Galili et al. (52), we observed that reversibly sickled cells (RSCs) were the predominant sickle RBC type in band 2, a mixture of RSCs and ISCs were found in band 4, and predominantly ISCs were found in band 6.

*Alteration of RBC MCHC values.* Normal RBCs were dehydrated or rehydrated by overnight incubation at 4°C in KPBS containing various concentrations of sucrose. Lateral and rotational mobility measurements were performed after the overnight incubation. An algorithmic extrapolation from the buffer osmolality was used to estimate MCHC values of RBCs in sucrose-containing buffers (60, 61); see Fig. 7 for these estimates.

Dense sickle RBCs were hypotonically swollen by incubation at room temperature for 1–2 h in 130–200-mosM buffers. Hypotonic solutions were generated by dilution of KPBS with distilled water and verification of pH at 7.4. Osmolalities were measured by using a freezing point depression osmometer (Osmette, Precision Systems Inc., Natick, MA). RBC swelling was predicted to be completed within 60 min of the start of incubation (60, 61). Osmotic swelling of dense sickle RBCs was confirmed by phase-contrast microscopy.

*Preparation of CO-saturated deoxygenated RBCs.* Carbon monoxide–saturated deoxygenated RBCs were produced by sealing a suspension of labeled RBCs in a Wheaton vial, passing humidified $N_2$ gas into the vial (without foaming) for 1 h, passing humidified CO gas over the cells for 1 h, and adding an enzyme oxygen scavenging system (described below) to complete the removal of oxygen. This protocol yielded RBCs in which all of the hemoglobin was liganded by CO and therefore in the R conformation.

*Lateral and rotational mobility measurements.* FPR was used to measure the lateral mobility of fluorescently labeled band 3, glycophorins, and phospholipids in membranes of intact RBCs (62). Briefly, a Gaussian laser beam was focused to a spot on a fluorescently labeled RBC in a fluorescence microscope. After a brief intense photobleaching pulse, recovery of fluorescence was monitored by periodic low-intensity pulses. Recovery resulted from the lateral diffusion of unbleached fluorophores into the bleached area. Nonlinear least-squares analysis (63) of fluorescence recovery data yielded both the diffusion

coefficient ($D$) and the fraction ($f$) of fluorescently labeled molecules that were free to diffuse on the time scale of the experiment (64).

PFD was used to measure the rotational mobility of eosin-labeled band 3 in membranes of intact RBCs. This technique combines the sensitivity of fluorescence detection with the long lifetime of excited triplet states (65, 66). Briefly, recovery of fluorescence after a ground state depletion pulse depended both on the triplet lifetime(s) of the fluorophore and on the rotational relaxation time(s) of band 3. In addition, the fraction of band 3 molecules that was rotationally immobile on the time scale of the experiment was obtained from the residual anisotropy of the fluorescence intensities excited by parallel and perpendicular probe beams (see references 66 and 67 for a complete description of the theory involved in PFD experiments). Using our laser microscope photometer, two exponential components of anisotropy decay and a residual anisotropy could be resolved, so data were fitted by nonlinear least-squares analysis to the equation

$$r(t) = r(\infty) + \alpha \cdot e^{(-t/\tau_1)} + \beta \cdot e^{(-t/\tau_2)},$$

where $r(t)$ is the anisotropy at time $t$, $r(\infty)$ is the residual anisotropy, and $\alpha$ and $\beta$ are the fractions of molecules with rotational correlation times $\tau_1$ and $\tau_2$, respectively. For anisotropy decay curves in which it was apparent that $\tau_1 < 40$ μs, $r(0)$ was set equal to the anisotropy value determined using eosin-labeled RBCs fixed with 1% glutaraldehyde. Band 3 in the membranes of fixed cells exhibited no rotational mobility and the anisotropy, typically 0.27–0.33, was time invariant. This procedure allowed the reliable determination of $\alpha$ but not $\tau_1$ in such cases.

EMA labels band 3 specifically at the external anion transport site of this protein (68, 69). EMA bound to band 3 in intact cells has multiple phosphorescence (triplet) lifetimes of 2.3, 0.4, and 0.04 ms (67), and a single fluorescence (singlet) lifetime of 2.99 ns (68). Despite the existence of multiple triplet lifetimes, however, our observation that band 3 exhibited multiple rotational correlation times indicates that several distinct classes of rotationally mobile band 3 coexist in the membrane (67). Since a uniformly rotating molecular species can theoretically give rise to two correlation times that differ by a factor of about four (67), our finding that the shorter and longer band 3 correlation times differed by nearly an order of magnitude suggests that these two values could not be due to a single class of rotational motion.

PFD experiments must be performed using deoxygenated solutions because $O_2$ effectively quenches the excited triplet state of eosin. Fluorescently labeled RBCs were deoxygenated by incubation in a glove box (818-GB; Plas-labs, Lansing, MI) set to the desired oxygen tension and by using an enzyme oxygen scavenging system. The enzyme scavenging system, which consisted of 50 U/ml glucose oxidase, 20 mM glucose, and $10^4$ U/ml catalase, served to reduce $O_2$ to $H_2O_2$ and $H_2O_2$ to $H_2O$ (66). The excess of catalase reduced significantly the lifetime of unwanted peroxides. To decrease further the potential for peroxide-mediated oxidative membrane damage, samples were first deoxygenated to 0.2% $O_2$ at room temperature for 60 min in the glove box and then treated with the enzyme oxygen scavenging system. Slides were prepared for PFD experiments by placing 3.2 μl of a 10% RBC suspension on a BSA-coated glass slide and using vacuum grease to seal a BSA-coated coverslip over the sample, all in the glove box. Lateral and rotational mobility measurements were performed within 6 h of fluorescent labeling. Results of PFD experiments using the enzyme scavenging system were identical to those using a more powerful glove box (Braun MB150M; courtesy of Dr. Christopher T. Walsh, Harvard Medical School, Boston, MA) to deoxygenate samples to 1 ppm $O_2$ without the use of scavenging enzymes.

*Time-resolved photon-counting laser microscope.* We designed and constructed a unique high-speed laser microscope photometer to measure lateral and rotational dynamics of RBC membrane proteins and lipids (Fig. 1). The instrument design was based on our apparatus described in Caulfield et al. (70) and modifications were adapted from the system described by Yoshida and Barisas (65). The light source for excitation, photoselection (PFD experiments), and photobleaching (FPR experiments) was a single 5-W argon ion laser (164-08; Spectra-Physics Inc., Mountain View, CA) tuned to 488 or 514 nm. Intensity

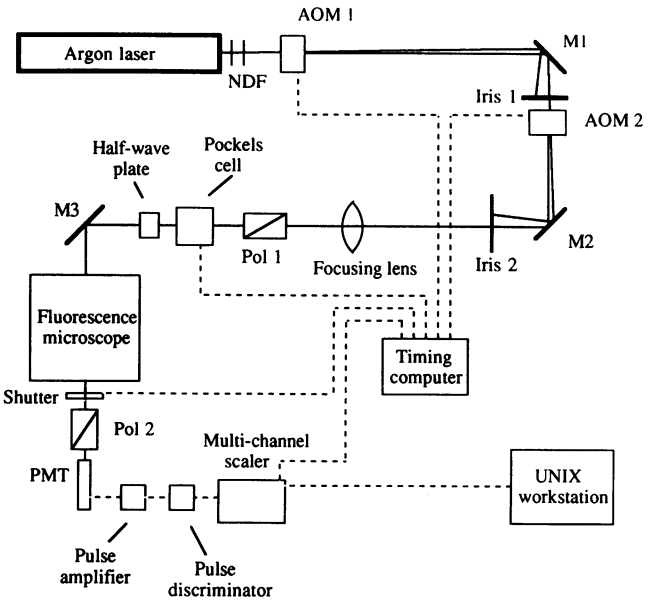


*Figure 1.* Time-resolved photon-counting laser microscope. Block diagram of apparatus for FPR and PFD measurements of lateral and rotational mobility of RBC membrane proteins and lipids. The use of two acousto-optic modulators provides the ability to set up the optical axis only once without need for time-consuming adjustments of multiple beans. The microscope consists of an Orthoplan/MPV3 with epi-illumination (F. Leitz Inc.) *AOM*, acousto-optic modulator; *M*, first surface mirror; *NDF*, neutral density filter; *PMT*, photon-counting photomultiplier tube; *Pol*, Glan-Taylor linear polarizer. See Methods for a complete description of the apparatus.

modulation by two computer-interfaced acousto-optic modulators (N35083-3; Newport Electro-Optics, Melbourne, FL) provided the three light intensities required for PFD and FPR experiments. Intensity-modulated light was passed through a Glan-Taylor polarizer (Oriel Corp. of America, Stratford, CT), a Pockels cell (1059; driven by a computer-interfaced 8025 high-voltage power supply; Lasermetrics Inc., Electro-Optics Div., Englewood, NJ), a 500-mm biconvex lens (Ealing Corp., Natick, MA), and a half wave plate before entering a research fluorescence microscope (Orthoplan/MPV-3, E. Leitz Inc., Rockleigh, NJ). Three iris diaphragms within the microscope eliminated stray light and unwanted reflections. The beam was directed onto the microscope stage by a 515-nm dichroic (for experiments that used the 488-nm laser line; E. Leitz Inc.) or a 563-nm DF55 dichroic (for experiments that used the 514-nm laser line; Omega Optical Inc., Brattleboro, VT) and was focused to a waist at the sample plane by an adjustable short focal length lens within the body of the microscope and a strain-free 25× 0.75 numerical aperture oil objective (for PFD experiments; E. Leitz Inc.) or a 100× 1.30 numerical aperture oil objective (for FPR experiments; E. Leitz Inc.). For PFD experiments a Gaussian beam of radius 30 μm was used to illuminate ~ 30 RBCs per measurement. For FPR experiments a beam of radius 0.8 μm was used and measurements were performed on individual RBCs. Sample temperature was controlled to ±0.5°C by a thermal microscope stage (model 80; E. Leitz Inc.).

Fluorescence emission from the sample was collected by the microscope objective and filtered by the dichroic, a 520-nm long pass filter, and a Glan-Taylor polarizer (Oriel Corp. of America). Emitted light was detected by a single-photon counting system consisting of a thermionically cooled (TE-104RF; Products for Research, Inc., Danvers, MA) photomultiplier tube (PMT) (Thorn EMI 9658RA) driven by a high-voltage power supply (model 1109; EG&G Princeton Applied Research, Princeton, NJ). An adjustable field diaphragm was used to discriminate against fluorescence from regions other than the RBC(s) of interest. PMT pulses were amplified and discriminated to 100 mV

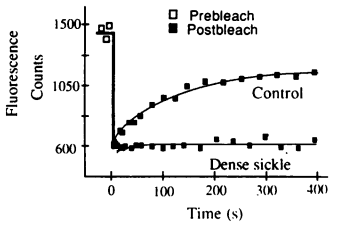


*Figure 2.* Typical fluorescence photobleaching recovery curves depicting lateral mobility of band 3 in unfractionated control and dense sickle RBCs at 37°C. Recovery of fluorescence was markedly reduced in the dense sickle cell sample, indicating lateral immobilization of band 3.

(model 1121A; EG&G Princeton Applied Research), and the resulting transistor-transistor logic pulses were fed into a multi-channel scaler (model 370; Nicolet Instrument Corp., Anal. Instrs. Div., Madison, WI). After each experiment data were sent to a computer workstation (Sun 386i/250) for processing. Experiment timing was controlled to $< 1$ μs by a custom programmed timing computer (Micro Linear Controls MLC-1A). During the intense FPR bleaching pulse a computer-interfaced electromechanical shutter (model SD-122B; Vincent Associates, Rochester, NY) was used to protect the PMT from excessive light. An electromechanical shutter was too slow and diodes in a commercial gating circuit (Thorn EMI GB1001A) generated too much electrical noise for use in PFD experiments, so a relatively weak and prolonged (5–10 μs) PFD photoselection pulse was used. Using such a pulse the PMT recovered within 25 μs so that rotational correlation times of ≥ 40 μs could be quantified. Suprasil-2 quartz slides and coverslips (Heraeus-Amersil, Inc., Sayreville, NJ) were used to reduce long-lived glass luminescence.

The photometer described above was ideal for FPR and PFD experiments on intact RBCs. Unlike other systems that require a relatively large phosphorescence signal from many cells to measure rotational correlation times, our apparatus used the sensitivity of fluorescence detection to allow performance of PFD measurements on ~ $10^2$ RBCs in one layer on a microscope slide. This instrumental design avoided the problem of inner filter effects experienced by cuvette systems, since the use of only a single layer of cells eliminated filtering by hemoglobin of excitation and emission light paths. Because of the small beam size and number of RBCs illuminated at one time in PFD experiments, data from 10 to 20 fields had to be accumulated to provide an acceptable signal/noise ratio. After ~ $10^3$ scans the fluorescence signal began to fade, probably because of fluorophore bleaching, and the beam was moved to a new field of RBCs.

## Results

*Band 3, glycophorin, and phospholipid mobility in control RBCs.* Lateral and rotational mobility measurements were performed on intact RBC membranes from seven patients with homozygous sickle cell disease and eight normal controls. Band 3 lateral and rotational mobility data were obtained from matched RBC samples on the same day.

Typical curves from FPR experiments on the lateral mobility of band 3 are shown in Fig. 2. Recovery curves were analyzed by nonlinear least-squares analysis to determine the average lateral diffusion rate and the fraction of laterally mobile molecules. Normal cells manifested a band 3 lateral diffusion rate ($D$) of 1–2 × $10^{-11}$ $cm^2/s$ and a fractional mobility ($f$) of 50 to 70%. Glycophorin and phospholipid lateral mobility measurements on control RBCs included diffusion coefficients of 2–5 and 200–400 × $10^{-11}$ $cm^2/s$ and fractional mobilities of 40–60 and 85–95%, respectively.

Typical sets of PFD fluorescence recovery data and the corresponding anisotropy curves are shown in Fig. 3. Anisotropy curves were fitted by nonlinear least-squares analysis to two exponential decays and a residual anisotropy. The exponential decays were used to determine two rotational correlation times and the fraction of band 3 molecules rotating with each of these correlation times, whereas the residual anisotropy was used to determine the fraction of rotationally immobile molecules. Control RBCs had three populations of band 3 molecules, including 15–30% rapidly rotating molecules ($\tau_1$, < 200 μs), 50–70% slowly rotating molecules ($\tau_2$, 1.5–3.0 ms), and 5–25% rotationally immobile molecules.

*Progressive lateral immobilization of band 3 and glycophorins in sickle and normal RBCs of increasing density.* Sickle RBCs were separated into six fractions according to buoyant density, and fractions characterized by MCHC values of 30, 37, and 42 g/dl were measured. As shown in Fig. 2, FPR experiments demonstrated large differences in lateral mobility between control and dense sickle samples. There were progressive decreases in the fractional mobilities of both band 3 and glycophorins as cell density increased. Protein fractional mobilities were similar to control values in the light sickle RBC fraction whereas mobilities were reduced by ~ 60% in the dense sickle RBC fraction (Fig. 4). The diffusion coefficients of the mobile band 3 and glycophorin molecules in all sickle RBC fractions were not significantly different from control values. Phospholipid diffusion coefficients in dense sickle RBCs were reduced by ~ 10% compared with control values, confirming results reported by Boullier et al. (71). Differences between the mag-

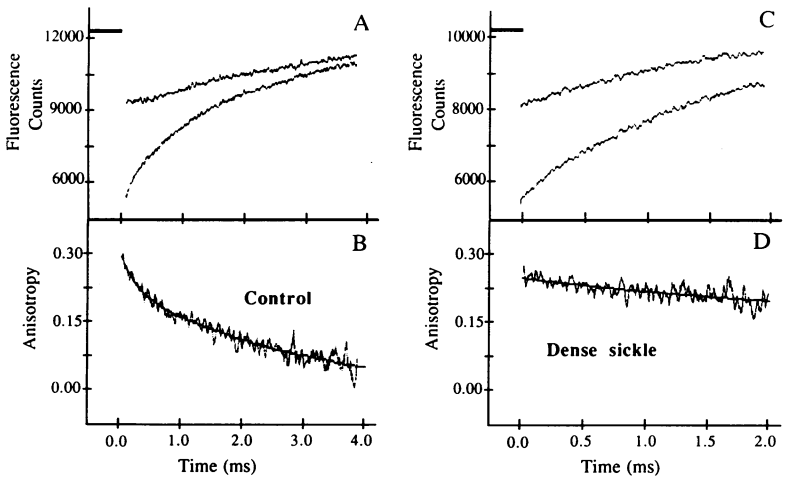


*Figure 3.* Typical polarized fluorescence depletion curves showing rotational mobility of band 3 in unfractionated control and dense sickle RBCs at 37°C. (*A* and *C*) Fluorescence recovery after polarized depletion (photoselection) of ground state fluorophores at $t = 0$. The upper curve resulted from a perpendicular orientation of depletion and probe beams whereas the lower curve resulted from a parallel alignment. $y$-axis, fluorescence counts per 5 μs channel. Data from ~ 300 cells were collected to produce the curves shown. (*B* and *D*) Decay of anisotropy calculated from the two fluorescence recovery curves in *A* and *C*, respectively. The decay of anisotropy curve could be resolved into two distinct rotationally mobile populations and a rotationally immobile component. The rotationally immobile component was markedly increased in the dense sickle cell sample.

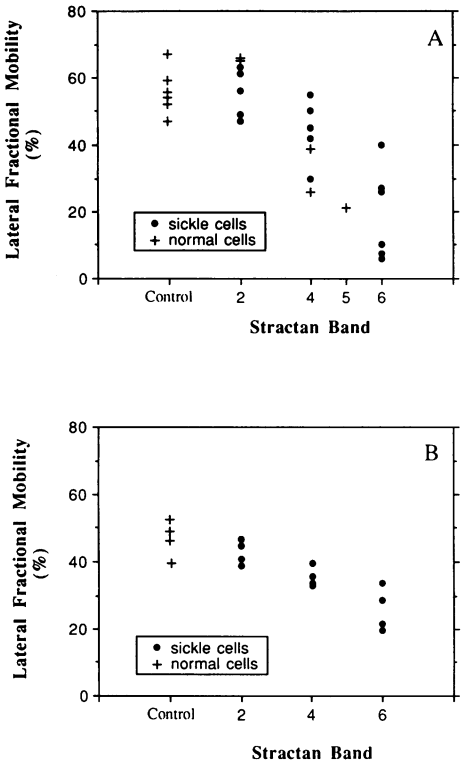


*Figure 4.* Lateral fractional mobilities of (*A*) band 3 and (*B*) glycophorins in normal and sickle RBCs at 37°C. Control samples represent unfractionated normal cells. Stractan bands 2, 4, and 6 contained light (band 2; MCHC = 30 g/dl), medium (band 4; MCHC = 37 g/dl), and dense (band 6; MCHC = 42 g/dl) cells. Each point represents the mean of 8 to 12 independent measurements from a single sample. Increasing cell density correlated with progressive lateral immobilization of band 3 and glycophorins.

nitudes of lipid diffusivities measured here and in reference 71 could be due to differences in the fluorescent lipid labels used.

Although the number of normal RBCs in the densest fractions was much smaller than the corresponding number of sickle RBCs (see also Fig. 1 of reference 52), normal RBCs separated according to buoyant density also showed a progressive decrease in the fractional mobility of band 3 with increasing cell density. The magnitude of this decrease was similar to that observed in density-separated sickle RBCs (Fig. 4 *A*).

*Progressive rotational immobilization of band 3 in sickle RBCs of increasing density.* The rotational mobility of band 3 was also measured in sickle RBC fractions characterized by MCHC values of 30, 37, and 42 g/dl. Control RBCs were not separated according to density for PFD measurements because insufficient numbers of normal cells migrated in Stractan bands 4, 5, and 6 for accurate measurements of rotational mobility. As shown in Fig. 3, PFD experiments demonstrated large differences in rotational mobility between control and dense sickle RBC samples. Light, medium, and dense sickle RBCs all manifested three distinct populations of band 3 molecules. $\tau_1$ and $\tau_2$ values in all sickle RBC fractions were identical to those observed in control RBCs. The relative proportions of band 3 molecules in the rapidly rotating, slowly rotating, and rotationally immobile populations were significantly different among the sickle RBC fractions, however. There was a progressive decrease in the fraction of rapidly rotating band 3 and progressive increases in the fractions of slowly rotating and rotationally immobile band 3 with increasing sickle RBC density (Figs. 5, 6). The fraction of rapidly rotating band 3 in control RBCs (23±5%, mean±SD) was similar to that in light sickle RBCs (24±5%) but much greater than that in dense sickle RBCs (5±7%) (Fig. 5). Conversely, the fraction of rotationally immobile band 3 in control RBCs (15±7%) was significantly less than that in light sickle RBCs (32±9%) and much less than that in dense sickle RBCs (56±5%) (Fig. 6). These data suggest that band 3 was progressively aggregated in sickle RBCs of increasing density. Further, the data show that a significant amount of aggregated band 3 was present in light as well as dense sickle RBCs. Since a significant increase in the fraction of rotationally immobile band 3 molecules was observed in light sickle RBCs, which had MCHC values (30 g/dl) less than those of control RBCs (34 g/dl), these changes in the aggregation state of band 3 were unlikely to be solely due to effects of increased RBC density.

*Inability of cellular dehydration to produce band 3 and glycophorin immobilization at MCHC values found in dense sickle and normal RBCs.* To investigate directly the relationship between RBC density changes and immobilization of band 3 and glycophorins, normal RBCs were osmotically

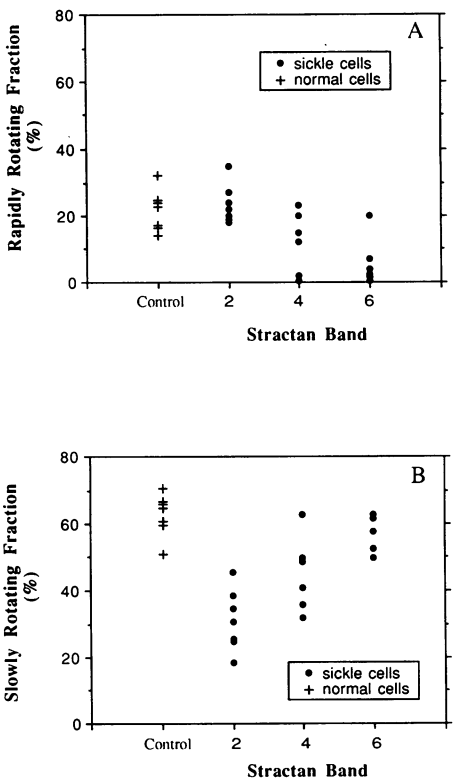


*Figure 5.* Rotational fractional mobilities of band 3 in normal and sickle RBCs at 37°C. Control samples represent unfractionated normal cells. Stractan bands 2, 4, and 6 contained light (MCHC = 30 g/dl), medium (MCHC = 37 g/dl), and dense (MCHC = 42 g/dl) sickle cells, respectively. Each point represents the fraction of band 3 molecules rotating with either (*A*) fast or (*B*) slow rotational correlation times in a single sample. Data were accumulated from ~ 300 cells per measurement.

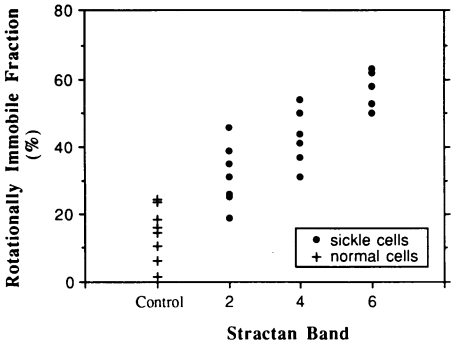


*Figure 6.* Rotationally immobile fraction of band 3 in normal and sickle RBCs at 37°C. Control samples represent unfractionated normal cells. Stractan bands 2, 4, and 6 contained light (MCHC = 30 g/dl), medium (MCHC = 37 g/dl), and dense (MCHC = 42 g/dl) sickle cells, respectively. Each point represents the fraction of band 3 molecules that were rotationally immobile on the time scale of the experiment ($\tau > 4$ ms) in a single sample. Data were accumulated from ~ 300 cells per measurement. Increasing sickle cell density correlated with progressive rotational immobilization of band 3.

shrunken by overnight incubation in KPBS with sucrose. Osmotic shrinkage did cause progressive lateral immobilization of both proteins (Fig. 7 *A*) and rotational immobilization of band 3 (Fig. 7 *B*) at buffer osmolalities > 450 mosM. Upon substitution of these incubation buffer conditions into two independently derived models of the relationship between the amount of sucrose added to a solution and the MCHC of RBCs incubated in that solution (60, 61), however, it was found that buffer osmolalities > 450 mosM corresponded to predicted MCHC values > 44 g/dl (Fig. 7). Dense sickle and normal RBCs, which had measured MCHC values of 38 to 44 g/dl, were therefore likely to have additional membrane abnormalities that caused transmembrane protein immobilization.

As a second test of the hypothesis that cell density was directly responsible for protein aggregation, dense sickle RBCs were osmotically swollen by incubation in hypotonic buffers of 200, 160, and 135 mosM. Osmotic swelling of dense sickle RBCs has been observed to produce a decrease in MCHC sufficient for cells to exhibit the spiculated sickling behavior characteristic of cells of lower density (72, 73). Only slight (5–10%) increases in the fractions of laterally mobile band 3 and glycophorins were observed upon incubation of dense sickle RBCs at 200 and 160 mosM, and sickle RBC lysis occurred at 135 mosM. In contrast, the density-dependent increases in the laterally immobile fractions of band 3 and glycophorins and in the rotationally immobile fraction of band 3 were entirely reversible upon rehydration of osmotically shrunken normal RBCs by incubation of cells in isotonic buffer (data not shown). These data suggest further that irreversible membrane alterations, rather than cellular dehydration, were responsible for the large immobile fractions of band 3 and glycophorins in dense sickle RBCs.

*Lack of effect of sickle RBC deoxygenation on band 3 mobility.* We attempted to compare the lateral and rotational mobilities of band 3 in oxygenated sickle RBCs with those in sickle RBCs deoxygenated under $N_2$ (which allows deoxyhemoglobin S to polymerize and morphologic sickling to occur) and in sickle RBCs deoxygenated under CO (which maintains hemoglobin S in the R conformation and therefore prevents hemoglobin polymerization and morphologic sickling). Concerning comparisons of band 3 lateral mobility, FPR experiments showed that the fractional mobility of band 3 was significantly decreased in eosin-labeled control RBCs incubated at $O_2$ tensions < 2 torr. This apparent immobilization of band 3 was not due to increased binding of deoxyhemoglobin A to the cytoplasmic domain of band 3, since the effect was not reversed by deoxygenation under CO instead of $N_2$. Rather, it appeared that the photobleaching of eosin generated reactive species that

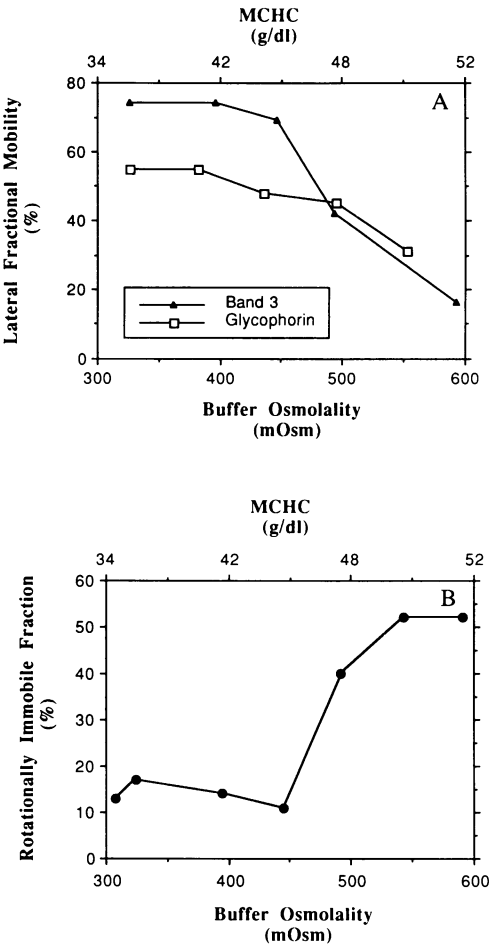


*Figure 7.* Lateral and rotational mobility of band 3 and glycophorins in osmotically shrunken normal RBCs. (*A*) Lateral fractional mobilities of band 3 and glycophorins in osmotically shrunken normal RBCs at 37°C. (*B*) Fraction of rotationally immobile band 3 in osmotically shrunken normal RBCs at 37°C. Cells were incubated overnight at 4°C in KPBS to which varying concentrations of sucrose were added. Buffer osmolalities were confirmed by using a freezing point depression osmometer. MCHC values were calculated as described in Methods. Error bars are omitted for clarity. Standard deviations were typically (*A*) ±15% and (*B*) ±30% of the value of the measurement. Dehydration of normal RBCs induced progressive immobilization of band 3 and glycophorins, but only at predicted MCHC values greater than those found in the dense sickle cell fraction. Further, whereas protein immobilization was reversible upon swelling of dehydrated normal cells in isotonic buffer, the immobilization associated with dense sickle cells was not reversible upon incubation of cells in hypotonic buffer.

were normally quenched by $O_2$ but could not be removed by $N_2$ or CO (Corbett, J. D., and D. E. Golan, manuscript submitted for publication). It was therefore not possible to interpret reliably the results of FPR experiments on deoxygenated eosin-labeled sickle RBCs.

Band 3 rotational mobility, in contrast, must be measured under deoxygenated conditions. Deoxygenation under CO instead of $N_2$ decreased by 10 to 20% the fraction of rotationally immobile band 3 in dense sickle RBCs and had no significant effect on the fraction of rotationally immobile band 3 in sickle RBCs of low and moderate density (data not shown). Stractan band 6 was composed largely of ISCs, and most ISCs do not undergo morphologic sickling. It is therefore unlikely that the effect of deoxygenation on band 3 rotational mobility was due to cellular shape change. Rather, it appears that deoxyhemoglobin S, which binds with higher affinity than oxyhemoglobin S to the cytoplasmic domain of band 3 (10, 56, 74), caused rotational immobilization of a minor fraction of band 3 molecules in deoxygenated dense sickle RBCs. Nonetheless, these observations further support the contention that dense sickle RBCs have, in addition to an increased MCHC value, irreversible membrane abnormalities that result in transmembrane protein immobilization.

## Discussion

Rapidly rotating, slowly rotating, and rotationally immobile forms of band 3 appear to coexist in the normal RBC membrane. The consistent observation of distinct, well-defined rotational populations suggests that equilibria exist among the various molecular states of band 3 in the membrane. Others have estimated that, at 37°C, 25–35% of band 3 molecules rotate with correlation times $\leq 150$ $\mu$s, 30–50% rotate with correlation times $\sim 3$ ms, and 25–35% are rotationally immobile on the time scale of the experiment (67, 69). Recent measurements with improved instrumentation indicate that about one-half of the rapidly rotating fraction of band 3 molecules rotate with correlation times of 25 to 30 $\mu$s (67). The latter population may represent band 3 dimers that rotate free of constraints other than the viscosity of the lipid bilayer. We find here that, in control RBCs, 15–30% of band 3 molecules rotate rapidly with correlation times of $< 200$ $\mu$s, 50–70% rotate slowly with correlation times of 1.5–3.0 ms, and 5–25% are rotationally immobile on the time scale of the experiment. These values are in good agreement with literature values for band 3 rotation in normal RBC membranes.

Sickle RBCs, like normal RBCs, have coexisting populations of rapidly rotating, slowly rotating, and rotationally immobile forms of band 3. The distribution of band 3 molecules among these populations is abnormal, however, in that an increase in the rotationally immobile form is seen in RBCs from all density fractions. Further, striking decreases in the rapidly rotating population and increases in the rotationally immobile population are directly related to increasing RBC density. The laterally immobile fraction of band 3 also increases with increasing cell density in both sickle and normal RBCs. Molecular mechanisms that have been shown to cause lateral immobilization of transmembrane proteins include direct binding interactions, steric hindrance interactions, membrane lipid domain formation, and protein aggregation or complex formation (75, 76). Any of these mechanisms could be consistent with our observations of cell density–dependent lateral immobilization of band 3 in sickle RBCs, since increased membrane-associated hemoglobin, altered membrane skeletal structure, and deranged phospholipid distribution have all been described in dense sickle RBCs (33).

The number of potential molecular mechanisms capable of mediating rotational immobilization is more restricted, however, since rotational mobility is sensitive to nanometer scale rather than micrometer scale dynamic interactions. Such interactions could include direct protein-binding interactions and protein aggregation or complex formation but would be unlikely to include steric hindrance interactions and lipid domain formation. In other studies, decreased steric hindrance interactions in spectrin-deficient RBCs were found to cause a significant increase in the lateral diffusion coefficient of band 3 but not to affect the rotational correlation times or the distribution of band 3 molecules among rapidly rotating, slowly rotating, and rotationally immobile populations (14, 15; Corbett, J. D., P. Agre, J. Palek, and D. E. Golan, manuscript submitted for publication). We find here that direct binding of deoxyhemoglobin S to band 3 causes only a minor degree of rotational immobilization of this transmembrane protein, since deoxygenated sickle RBCs exposed to $N_2$ manifest band 3 rotational mobility parameters similar to those exposed to CO. Our data suggest instead that band 3 is progressively and irreversibly aggregated in sickle and normal RBCs of increasing density and that light as well as dense sickle RBCs have increased amounts of aggregated band 3. One brief report of band 3 rotational diffusion in unfractionated sickle RBCs has recently appeared. Two correlation times of 0.2 and 4.7 ms were reported, in qualitative agreement with our data (77).

Dense sickle and normal RBCs are by definition dehydrated. Cellular dehydration could lead to alterations in membrane organization and thereby to changes in integral membrane protein mobility. We tested this hypothesis in the present studies and conclude for the following reasons that cellular dehydration was not responsible for the observed immobilization of band 3 and glycophorins in dense sickle and normal RBCs. First, decreases in both lateral and rotational mobility occur in osmotically shrunken control RBCs only at MCHC values $> 44$ g/dl. If increased RBC density caused protein aggregation directly, then decreased mobility should have been seen in control RBCs at MCHC values of 38–44 g/dl. Second, mobility decreases in osmotically shrunken control RBCs are completely reversible upon removal of the shrunken cells into isotonic buffer. In contrast, osmotic swelling does not reverse the immobilization of band 3 in dense sickle cells. It appears, then, that irreversible membrane alterations are primarily responsible for increased band 3 and glycophorin aggregation in dense sickle and normal RBCs.

Progressive and irreversible band 3 aggregation in sickle RBCs of increasing density could be mediated by known biochemical alterations in sickle RBC membranes. Decreased high affinity binding of ankyrin to spectrin (78) and of band 3 to ankyrin (Platt, O. S., personal communication) could allow the formation of large band 3 clusters that are rotationally as well as laterally immobile. Increased binding of hemoglobin (79) and hemichrome (80) at the inner membrane surface could facilitate oxidative cross-linking within such clusters, promoting further immobilization. Finally, irreversible band 3 immobilization could result from the relative inability of older

RBCs to prevent and repair damage due to oxidative stress (41, 42).

Hemolysis of dense sickle and senescent normal RBCs may be mediated by increased binding of autologous IgG to dense RBCs (52–57). Phenylhydrazine-induced hemichrome formation also induces increased binding of autologous IgG to the membrane; the most prominent sites of IgG binding correlate with areas of Heinz body formation and band 3 aggregation (55). Band 3 aggregation, presumably initiated by hemichrome binding to band 3 and/or oxidative damage to the membrane, has been postulated to be the molecular event responsible for increased IgG binding and subsequent removal of dense sickle and senescent normal cells from the circulation (55). The epitope recognized by the antibody is not clearly defined; candidate structures include an altered form of band 3 (81, 82), abnormally exposed galactosyl residues (46, 83, 84), and clustered band 3 molecules (27, 48, 50). Our data support the hypothesis that band 3 aggregation provides an important surface marker for RBC removal from the circulation.

The fractional mobility of glycophorins, like that of band 3, decreases progressively with increasing sickle RBC density. This observation suggests that glycophorins may be aggregated in dense sickle RBCs, although other molecular mechanisms could also mediate lateral immobilization (see above). Increased RBC adhesion to vascular endothelial cells has been postulated to result from clustering of negatively charged glycophorin-linked sialic acid moieties at the RBC surface (45, 85).

The present studies of lateral and rotational mobility were performed on intact RBCs using our time-resolved photon-counting laser microscope. Intact cells are likely to be more physiologic than ghost membrane preparations in elucidating molecular alterations that mediate removal of dense sickle and normal RBCs from the circulation. Band 3 lateral mobility has been studied in both RBC ghosts and intact cells (12, 13, 17, 64, 86). Whereas band 3 mobility in intact normal RBCs under physiologic conditions is relatively consistent from study to study, lateral mobility in ghost membranes is highly variable. Fractional mobilities ranging from 0 to 70% and diffusion coefficients from 0 to $80 \times 10^{-11}$ $cm^2/s$ have been reported (12, 13, 87–89). We have observed that small changes in experimental conditions can dramatically affect protein lateral mobility in RBC ghost membranes (data not shown). Previous studies of band 3 rotational mobility have been performed on macroscopic samples of RBC ghost membranes in cuvette-based systems (11, 18, 66, 67, 90–95). In one recent study the rotational mobility of band 3 was found to be similar in RBC ghosts and intact cells (67); this similarity may be fortuitous. Since RBC ghosts produced by hypotonic lysis may have altered interactions between integral membrane proteins and membrane skeletal proteins, dynamic measurements on intact cells are likely to provide a more accurate assessment of the physical states of band 3 and glycophorins in normal and abnormal RBC membranes.

In summary, we have used lateral and rotational mobility measurements to elucidate alterations in the physical states of band 3 and glycophorins in dense sickle and normal RBCs. Both transmembrane proteins appear to be progressively and irreversibly aggregated in RBCs of increased density. Band 3 clustering in particular may serve as the primary molecular signal for the removal of dense sickle RBCs (mainly ISCs) and dense normal RBCs (i.e., senescent cells) from the circulation.

## Acknowledgments

We thank Dr. Kenneth Bridges for referrals of patients with sickle cell anemia, the patients for generous donations of blood, and Dr. Alan Kleinfeld for the multiexponential curve-fitting program.

This work was supported by National Institutes of Health grants HL-15157 and HL-32854 (D. E. Golan). J. D. Corbett was supported by NIH training grant HL-07623 for portions of this work.

## References

1. Hebbel, R. P., R. S. Schwartz, and N. Mohandas. 1985. The adhesive sickle erythrocyte: cause and consequence of abnormal interactions with endothelium, monocytes/macrophages and model membranes. *Clin. Haematol.* 14:141–161.

2. Bennett, V. 1985. The membrane skeleton of human erythrocytes and its implications for more complex cells. *Annu. Rev. Biochem.* 54:273–304.

3. Steck, T. L. 1974. The organization of proteins in the human red blood cell membrane. A review. *J. Cell Biol.* 62:1–19.

4. Cabantchik, Z. I., P. A. Knauf, and A. Rothstein. 1978. The anion transport system of the red blood cell. The role of membrane protein evaluated by the use of 'probes'. *Biochim. Biophys. Acta.* 515:239–302.

5. Marchesi, V. T., H. Furthmayer, and M. Tomita. 1976. The red cell membrane. *Annu. Rev. Biochem.* 45:667–698.

6. Low, P. S. 1986. Structure and function of the cytoplasmic domain of band 3: center of erythrocyte membrane-peripheral protein interactions. *Biochim. Biophys. Acta.* 864:145–167.

7. Low, P. S., B. M. Willardson, N. Mohandas, M. Rossi, and S. Shohet. 1991. Contribution of the band 3-ankyrin interaction to erythrocyte membrane mechanical stability. *Blood.* 77:1581–1586.

8. Chasis, J. A., and S. B. Shohet. 1987. Red cell biochemical anatomy and membrane properties. *Annu. Rev. Physiol.* 49:237–248.

9. Sheetz, M. P. 1983. Membrane skeletal dynamics: role in modulation of red cell deformability, mobility of transmembrane proteins, and shape. *Semin. Hematol.* 20:175–188.

10. Sheetz, M. P., and D. E. Koppel. 1979. Membrane damage caused by irradiation of fluorescent concanavalin A. *Proc. Natl. Acad. Sci. USA.* 76:3314–3317.

11. Tsuji, A., K. Kawasaki, and S. Ohnishi. 1988. Regulation of band 3 mobilities in erythrocyte ghost membranes by protein association and cytoskeletal meshwork. *Biochemistry.* 27:7447–7452.

12. Tsuji, A., and S. Ohnishi. 1986. Restriction of the lateral motion of band 3 in the erythrocyte membrane by the cytoskeletal network: dependence on spectrin association state. *Biochemistry.* 25:6133–6138.

13. Golan, D. E., and W. Veatch. 1980. Lateral mobility of band 3 in the human erythrocyte membrane studied by fluorescence photobleaching recovery: evidence for control by cytoskeletal interactions. *Proc. Natl. Acad. Sci. USA.* 77:2537–2541.

14. Golan, D. E., J. Palek, and P. C. Agre. 1990. Red cell membrane spectrin content regulates band 3 and glycophorin lateral diffusion. *Blood.* 76:8a.

15. Corbett, J. D., P. Agre, and D. E. Golan. 1992. Lateral and rotational mobility of band 3 in severe, recessively inherited spectrin deficient HS: evidence for differential control of mobility. *Annu. Biophys. Soc. Meet., Houston, TX.* Feb 9–13, 1992.

16. Corbett, J. D., H. S. Thatte, P. Jarolim, C. M. Cohen, J. Delaunay, Y. Yawata, J. T. Prchal, J. Palek, and D. E. Golan. 1992. Band 3 rotational and lateral mobility are regulated by different molecular interactions: a comparative study in normal and abnormal red blood cells. *Annu. Biophys. Soc. Meet., Houston, TX.* Feb 9–13, 1992.

17. Koppel, D. E., M. P. Sheetz, and M. Schindler. 1981. Matrix control of protein diffusion in biological membranes. *Proc. Natl. Acad. Sci. USA.* 78:3576–3580.

18. Nigg, E. A., and R. J. Cherry. 1980. Anchorage of a band 3 population at the erythrocyte cytoplasmic membrane surface: protein rotational diffusion measurements. *Proc. Natl. Acad. Sci. USA.* 77:4702–4706.

19. Embury, S. H. 1986. The clinical pathophysiology of sickle cell disease. *Annu. Rev. Med.* 37:361–376.

20. Havell, T. C., D. Hillman, and L. S. Lessin. 1978. Deformability characteristics of sickle cells by microelastimetry. *Am. J. Hematol.* 4:9–16.

21. Zachowski, A., C. T. Craescu, F. Galacteros, and P. F. Devaux. 1985. Abnormality of phospholipid transverse diffusion in sickle erythrocytes. *J. Clin. Invest.* 75:1713–1717.

22. Middlekoop, E., B. H. Lubin, E. M. Bevers, J. A. F. Op den Kamp, P. Comfurius, D. T. Y. Chiu, R. F. A. Zwaal, L. L. M. van Deenen, and B. Roelofsen. 1988. Studies on sickled erythrocytes provide evidence that the asymmetric distribution of phosphatidylserine in the red cell membrane is maintained by

both ATP-dependent translocation and interaction with membrane skeletal proteins. *Biochim. Biophys. Acta.* 937:281–288.

23. Lubin, B., D. Chiu, J. Bastacky, B. Roelofsen, and L. L. M. Van Deenen. 1981. Abnormalities in membrane phospholipid organization in sickled erythrocytes. *J. Clin. Invest.* 67:1643–1649.

24. Devaux, P. F. 1991. Static and dynamic lipid asymmetry in cell membranes. *Biochemistry.* 30:1163–1173.

25. Chiu, D., and B. Lubin. 1979. Erythrocyte membrane lipid reorganization during the sickling process. *Br. J. Haematol.* 41:223–234.

26. Lux, S. E., K. M. John, and M. J. Karnovsky. 1976. Irreversible deformation of the spectrin-actin lattice in irreversibly sickled cells. *J. Clin. Invest.* 58:955–963.

27. Waugh, S. M., B. M. Willardson, R. Kannah, R. J. Labotka, and P. S. Low. 1986. Heinz bodies induce clustering of band 3, glycophorin, and ankyrin in sickle cell erythrocytes. *J. Clin. Invest.* 78:1155–1160.

28. Hebbel, R. P., O. Yamada, C. F. Moldow, H. S. Jacob, J. G. White, and J. W. Eaton. 1980. Abnormal adherence of sickle erythrocytes to cultured vascular endothelium. Possible mechanism for microvascular occlusion in sickle cell disease. *J. Clin. Invest.* 65:154–160.

29. Clark, L. J., L. S. Chan, D. R. Powars, and R. F. Baker. 1981. Negative charge distribution and density on the surface of oxygenated normal and sickle red cells. *Blood.* 57:675–678.

30. Shaklai, N., V. S. Sharma, and H. M. Ranney. 1981. Interaction of sickle cell hemoglobin with erythrocyte membranes. *Proc. Natl. Acad. Sci. USA.* 78:65–68.

31. Jain, S. K., and S. B. Shohet. 1984. A novel phospholipid in irreversibly sickled cells: evidence for in vivo peroxidative membrane damage in sickle cell disease. *Blood.* 63:362–367.

32. Hebbel, R. P., J. W. Eaton, M. H. Balasingam, and M. H. Steinberg. 1982. Spontaneous oxygen radical generation by sickle erythrocytes. *J. Clin. Invest.* 70:1253–1259.

33. Hebbel, R. P. 1991. Beyond hemoglobin polymerization: the red blood cell membrane and sickle disease pathophysiology. *Blood.* 77:214–237.

34. Tosteson, D. C., E. Shea, and R. C. Darling. 1952. Potassium and sodium of red blood cells in sickle cell anemia. *J. Clin. Invest.* 31:406–411.

35. Tosteson, D. C., E. Carlsen, and E. T. Dunham. 1955. The effects of sickling on ion transport. *J. Gen. Physiol.* 39:31–53.

36. Eaton, J. W., T. D. Skelton, H. S. Swofford, C. F. Kolpin, and H. S. Jacob. 1973. Elevated erythrocyte calcium in sickle cell disease. *Nature (Lond.).* 246:105–106.

37. Nash, G. B., and S. J. Wyard. 1980. Shape of ageing erythrocytes. *Biorheology.* 17:479–484.

38. Winterbourn, C. C., and R. D. Batt. 1970. The uptake of plasma fatty acids into human red cells and its relationship to cell age. *Biochim. Biophys. Acta.* 202:9–20.

39. Seaman, G. V. F., R. J. Knox, F. J. Nordt, and D. H. Regan. 1977. Red cell aging. I. Surface charge density and sialic acid content of density-fractionated human erythrocytes. *Blood.* 50:1001–1011.

40. Cohen, N. S., J. E. Ekholm, M. G. Luthra, and D. G. Hanahan. 1976. Biochemical characterization of density-separated human erythrocytes. *Biochim. Biophys. Acta.* 419:229–242.

41. Glass, G. A., H. Gershon, and D. Gershon. 1983. The effect of donor and cell age on several characteristics of rat erythrocytes. *Exp. Hematol. (NY).* 11:987–995.

42. Imanishi, H., T. Kakai, T. Abe, and T. Takino. 1985. Glutathione metabolism in red cell aging. *Mech. Ageing Dev.* 32:57–62.

43. Kadlubowski, M. 1978. The effect of in-vivo ageing of the human erythrocyte on the protein of the plasma membrane. A characterisation. *Int. J. Biochem.* 9:67–78.

44. Campwala, H. Q., and J. F. Desforges. 1982. Membrane-bound hemichrome in density-separated cohorts of normal (AA) and sickled (SS) cells. *J. Lab. Clin. Med.* 99:25–28.

45. Marikovsky, Y., and D. Danon. 1969. Electron microscope analysis of young and old red blood cells stained with colloidal iron for surface charge evaluation. *J. Cell Biol.* 43:1–7.

46. Alderman, E. M., H. H. Fudenberg, and R. E. Lovins. 1981. Isolation and characterization of an age-related antigen present on senescent human red blood cells. *Blood.* 58:341–349.

47. Galili, U., I. Flechner, A. Knyszynski, D. Danon, and E. A. Rachmilewitz. 1986. The natural anti-alpha-galactosyl IgG on human normal senescent red blood cells. *Br. J. Haematol.* 62:317–324.

48. Green, G. A., M. M. Rehn, and V. K. Kalra. 1985. Cell-bound autologous immunoglobulin in erythrocyte subpopulations from patients with sickle cell disease. *Blood.* 65:1127–1133.

49. Kay, M. M. B. 1975. Mechanism of removal of senescent cells by human macrophages in situ. *Proc. Natl. Acad. Sci. USA.* 72:3521–3525.

50. Khansari, N., G. F. Springer, E. Merler, and H. H. Fudenberg. 1983. Mechanisms for the removal of senescent human erythrocytes from circulation: specificity of the membrane-bound immunoglobulin G. *Mech. Ageing Dev.* 21:49–58.

51. Smalley, C. E., and E. M. Tucker. 1983. Blood group A antigen site distribution and immunoglobulin binding in relation to red cell age. *Br. J. Haematol.* 54:210–219.

52. Galili, U., M. R. Clark, and S. B. Shohet. 1986. Excessive binding of natural anti-alpha-galactosyl immunoglobin G to sickle erythrocytes may contribute to extravascular cell destruction. *J. Clin. Invest.* 77:27–33.

53. Kay, M. M. B. 1984. Localization of senescent cell antigen on band 3. *Proc. Natl. Acad. Sci. USA.* 81:5753–5757.

54. Kay, M. M. B., S. R. Goodman, K. Sorensen, C. F. Whitfield, P. Wong, L. Zaki, and V. Rudloff. 1983. Senescent cell antigen is immunologically related to band 3. *Proc. Natl. Acad. Sci. USA.* 80:1631–1635.

55. Low, P. S., S. M. Waugh, K. Zinke, and D. Drenckhahn. 1985. The role of hemoglobin denaturation and band 3 clustering in red blood cell aging. *Science (Wash. DC).* 227:531–533.

56. Walder, J. A., R. Chatterjee, T. L. Steck, P. S. Low, G. F. Musso, E. T. Kaiser, P. H. Rogers, and A. Arnone. 1984. The interaction of hemoglobin with the cytoplasmic domain of band 3 of the human erythrocyte membrane. *J. Biol. Chem.* 259:10238–10246.

57. Waugh, S. M., and P. S. Low. 1985. Hemichrome binding to band 3: nucleation of Heinz bodies on the erythrocyte membrane. *Biochemistry.* 24:34–39.

58. Mohandas, N., and W. Groner. 1989. Cell membrane and volume changes during red cell development and aging. *Ann. NY Acad. Sci.* 554:217–224.

59. Corash, L., B. Shafer, and M. Perlow. 1978. Heterogeneity of human whole blood platelet subpopulations. II. Use of a subhuman primate model to analyze the relationship between density and platelet age. *Blood.* 52:726–734.

60. Freedman, J. C., and J. E. Hoffman. 1979. Ionic and osmotic equilibria of human red blood cells treated with nystatin. *J. Gen. Physiol.* 74:157–185.

61. Lew, V. L., and R. M. Bookchin. 1986. Volume, pH, and ion-content regulation in human red cells: analysis of transient behavior with an integrated model. *J. Membr. Biol.* 92:57–74.

62. Axelrod, D., D. E. Koppel, J. Schlessinger, E. Elson, and W. W. Webb. 1976. Mobility measurements by analysis of fluorescence photobleaching recovery kinetics. *Biophys. J.* 16:1055–1069.

63. Bevington, P. R. 1969. Data Reduction and Error Analysis for the Physical Sciences. McGraw-Hill Inc., New York. 336 pp.

64. Golan, D. E., C. S. Brown, C. M. L. Cianci, S. T. Furlong, and J. P. Caulfield. 1986. Schistosomula of *Schistosoma mansoni* use lysophosphatidylcholine to lyse adherent red blood cells and immobilize red cell membrane components. *J. Cell Biol.* 103:819–828.

65. Yoshida, T. M., and B. G. Barisas. 1986. Protein rotational motion in solution measured by polarized fluorescence depletion. *Biophys. J.* 50:41–53.

66. Johnson, P., and P. B. Garland. 1981. Depolarization of fluorescence depletion. *FEBS (Fed. Eur. Biochem. Soc.) Lett.* 132:252–256.

67. Matayoshi, E. D., and T. M. Jovin. 1991. Rotational diffusion of band 3 in erythrocyte membranes. 1. Comparison of ghosts and intact cells. *Biochemistry.* 30:3525–3538.

68. Macara, I. G., S. Kuo, and L. C. Cantley. 1983. Evidence that inhibitors of anion exchange induce a transmembrane conformational change in band 3. *J. Biol. Chem.* 258:1785–1792.

69. Nigg, E. A., and R. J. Cherry. 1979. Influence of temperature and cholesterol on the rotational diffusion of band 3 in the human erythrocyte membrane. *Biochemistry.* 18:3457–3465.

70. Caulfield, J. P., C. Chiang, P. W. Yacono, L. A. Smith, and D. E. Golan. 1991. Low density lipoproteins bound to *Schistosoma mansoni* do not alter the rapid lateral diffusion or shedding of lipids in the outer surface membrane. *J. Cell Sci.* 99:167–173.

71. Boullier, J. A., B. A. Brown, J. C. Bush, and B. G. Barisas. 1986. Lateral mobility of a lipid analog in the membrane of irreversible sickle erythrocytes. *Biochim. Biophys. Acta.* 856:301–309.

72. Clark, M. R., J. C. Guatelli, N. Mohandas, and S. B. Shohet. 1980. Influence of red cell water content on the morphology of sickling. *Blood.* 55:823–830.

73. Mohandas, N., M. E. Rossi, and M. R. Clark. 1986. Association between morphologic distortion of sickle cells and deoxygenation-induced cation permeability increase. *Blood.* 68:450–454.

74. Chetrite, G., and R. Cassoly. 1985. Affinity of hemoglobin for the cytoplasmic fragment of human erythrocyte membrane band 3. *J. Mol. Biol.* 185:639–644.

75. Nicolson, G. L. 1976. Transmembrane control of the receptors on normal and tumor cells. I. Cytoplasmic influence over surface components. *Biochim. Biophys. Acta.* 457:57–108.

76. Elson, E. L. 1986. Membrane dynamics studied by fluorescence correlation spectroscopy and photobleaching recovery. *Soc. Gen. Physiol. Ser.* 40:367–383.

77. Korkidis, K. 1989. Use of time-resolved phosphorescence spectroscopy to

study protein mobility in normal and abnormal red blood cells. *Spectroscopy (Ott)*. 2:1–3.

78. Bennett, V. 1978. Purification of an active proteolytic fragment of the membrane attachment site for human erythrocyte spectrin. *J. Biol. Chem.* 253:2292–2299.

79. Hebbel, R. P. 1990. The sickle erythrocyte in double jeopardy: autoxidation and iron decompartmentalization. *Semin. Hematol.* 27:51–69.

80. Kuross, S. A., B. H. Rank, and R. P. Hebbel. 1988. Excess heme in sickle erythrocyte inside-out membranes: possible role in thiol oxidation. *Blood.* 71:876–882.

81. Kay, M. M. B., G. J. C. Bosman, and C. Lawrence. 1988. Functional topography of band 3: specific structural alteration linked to functional aberrations in human erythrocytes. *Proc. Natl. Acad. Sci. USA.* 85:492–496.

82. Kay, M. M. B., N. Flowers, J. Goodman, and G. Bosman. 1989. Alteration in membrane protein band 3 associated with accelerated erythrocyte aging. *Proc. Natl. Acad. Sci. USA.* 86:5834–5838.

83. Aminoff, D. 1988. The role of sialoglycoconjugates in the aging and sequestration of red cells from circulation. *Blood Cells (NY).* 14:229–247.

84. Galili, U., A. Korkesh, I. Kahane, and E. A. Rachmilewitz. 1983. Demonstration of a natural antigalactosyl IgG antibody on thalassemic red blood cells. *Blood.* 61:1258–1264.

85. Hebbel, R. P., M. A. B. Boogaerts, J. W. Eaton, and M. H. Steinberg. 1980. Erythrocyte adherence to endothelium in sickle-cell anemia. A possible determinant of disease severity. *N. Engl. J. Med.* 302:992–995.

86. Sheetz, M. P., M. Schindler, and D. E. Koppel. 1980. Lateral mobility of integral membrane proteins is increased in spherocytic erythrocytes. *Nature (Lond.).* 285:510–512.

87. Golan, D. E. 1989. Red blood cell membrane protein and lipid diffusion. *In* Red Blood Cell Membranes. P. Agre and J. C. Parker, editors. Marcel Dekker, New York. 367–400.

88. Golan, D. E. 1982. Dynamic interactions in the human erythrocyte membrane: studies on the lateral mobility of band 3, phospholipid, and cholesterol. Ph.D. thesis. Yale University, New Haven, CT.

89. Peters, R., J. Peters, K. H. Tews, and W. Bahr. 1974. A microfluorimetric study of translational diffusion in erythrocyte membranes. *Biochim. Biophys. Acta.* 367:282–294.

90. Clague, M. J., J. P. Harrison, and R. J. Cherry. 1989. Cytoskeletal restraints of band 3 rotational mobility in human erythrocyte membranes. *Biochim. Biophys. Acta.* 981:43–50.

91. Matayoshi, E. D., W. H. Sawyer, and T. M. Jovin. 1991. Rotational diffusion of band 3 in erythrocyte membranes. 2. Binding of cytoplasmic enzymes. *Biochemistry.* 30:3538–3543.

92. Nigg, E. A., C. G. Gahmberg, and R. J. Cherry. 1980. Rotational diffusion of band 3 proteins in membranes from En(a-) and neuraminidase-treated normal human erythrocytes. *Biochim. Biophys. Acta.* 600:636–642.

93. Muhlebach, T., and R. J. Cherry. 1982. Influence of cholesterol on the rotation and self-association of band 3 in the human erythrocyte membrane. *Biochemistry.* 21:4225–4228.

94. Tilley, L., M. Foley, R. F. Anders, A. R. Dluzewski, W. B. Gratzer, G. L. Jones, and W. H. Sawyer. 1990. Rotational dynamics of the integral membrane protein, band 3, as a probe of the membrane events associated with *Plasmodium falciparum* infections of human erythrocytes. *Biochim. Biophys. Acta.* 1025:135–142.

95. Tilley, L., G. B. Nash, G. L. Jones, and W. H. Sawyer. 1991. Decreased rotational diffusion of band 3 in melanesian ovalocytes from Papua, New Guinea. *J. Membr. Biol.* 121:59–66.